



THE UNIVERSITY *of* EDINBURGH

Edinburgh Research Explorer

A unified resource and configurable model of the synapse proteome and its role in disease

Citation for published version:

Sorokina, O, Mclean, C, Croning, MDR, Heil, KF, Wysocka, E, He, X, Sterratt, D, Grant, SGN, Simpson, TI & Armstrong, JD 2021, 'A unified resource and configurable model of the synapse proteome and its role in disease', *Scientific Reports*, vol. 11, no. 1. <https://doi.org/10.1038/s41598-021-88945-7>

Digital Object Identifier (DOI):

[10.1038/s41598-021-88945-7](https://doi.org/10.1038/s41598-021-88945-7)

Link:

[Link to publication record in Edinburgh Research Explorer](#)

Document Version:

Publisher's PDF, also known as Version of record

Published In:

Scientific Reports

General rights

Copyright for the publications made accessible via the Edinburgh Research Explorer is retained by the author(s) and / or other copyright owners and it is a condition of accessing these publications that users recognise and abide by the legal requirements associated with these rights.

Take down policy

The University of Edinburgh has made every reasonable effort to ensure that Edinburgh Research Explorer content complies with UK legislation. If you believe that the public display of this file breaches copyright please contact openaccess@ed.ac.uk providing details, and we will remove access to the work immediately and investigate your claim.





OPEN

A unified resource and configurable model of the synapse proteome and its role in disease

Oksana Sorokina^{1✉}, Colin Mclean^{1✉}, Mike D. R. Croning², Katharina F. Heil^{1,4}, Emilia Wysocka¹, Xin He^{1,5,6}, David Sterratt¹, Seth G. N. Grant^{2,5}, Thomas I. Simpson^{1,5} & J. Douglas Armstrong^{1,3,5}

Genes encoding synaptic proteins are highly associated with neuronal disorders many of which show clinical co-morbidity. We integrated 58 published synaptic proteomic datasets that describe over 8000 proteins and combined them with direct protein–protein interactions and functional metadata to build a network resource that reveals the shared and unique protein components that underpin multiple disorders. All the data are provided in a flexible and accessible format to encourage custom use.

At neuronal synapses, the proteomes in presynaptic and postsynaptic compartments form complex and highly dynamic molecular networks. These networks mediate signal transduction and plasticity processes that underpin normal (and abnormal) information processing in the brain. We systematically curated proteomic datasets dating from 2000 to 2020, to produce a comprehensive index of the proteins (and their genes) expressed at the mammalian synapse (see Methods for details). This resulted in 58 papers, which when combined, describe a landscape of 8087 synaptic genes.

The set includes 29 post synaptic proteome (PSP) studies (2000 to 2019) contributing a total of 5560 mouse and human unique gene identifiers; 18 presynaptic studies (2004 to 2020) describe 2772 unique human and mouse gene IDs, and 11 studies that span the whole synaptosome and report 7198 unique genes (Table 1, Supplementary Table 1).

Each study was annotated with relevant metadata including GO function, disease association and cross-ref to SynGo. Orthologues were mapped across human, mouse and rat and each mapped onto stable identifiers (MGI, Entrez and Uniprot).

High throughput proteomic techniques are powerful, but they are noisy, and contamination is always a concern. A large number (2091 for PSP and 1434 for presynapse, Fig. 1A,B) of proteins have been observed just once. While single hits may be accounted for lack of sensitivity with low abundance molecules, it could also indicate the presence of false positive components brought in by experimental uncertainty.

The rate of growth with respect to newly discovered proteins for PSP appears to be slowing (Fig. 1C,E) and therefore there is now an opportunity to define a more reliable subset. Following the approach described in¹¹, we selected genes found in two or more independent studies to designate the “consensus” PSP. This resulted in 3,438 genes, which is ~7 times larger than reported by¹¹ and described a subset of synaptic proteins for which have higher confidence. In this subset we observe the increment of new genes per year decreases after 2008 and drops completely after 2014 (Fig. 1C). Based on this, we predict a total number of consensus PSP genes found to be 3499 (Fig. 1G) by year 2023 which, when compared to the current number indicates that our knowledge on PSP components, based on currently available methodologies, is close to saturation.

It is different for the presynaptic compartment, where the recent trend in newly identified genes indicates that saturation has not been achieved yet (Fig. 1D,F). For instance, the latest study by Taoufiq et al.⁴⁷ brought in over 400 new genes to our presynaptic list.

The overlap of proteins found in pre- and post-synaptic datasets, and proteins identified in synaptosomal studies is shown at Fig. 1H and Fig. 1 in Supplementary Methods.

To reconstruct protein–protein interaction (PPI) networks for the pre- and post-synaptic proteomes we used human PPI data filtered for the highest confidence direct and physical interactions from BioGRID⁵⁸, Intact⁵⁹ and

¹The School of Informatics, University of Edinburgh, Edinburgh, UK. ²Centre for Clinical Brain Sciences, University of Edinburgh, Edinburgh, UK. ³Computational Biomedicine Institute (IAS-5 / INM-9), Forschungszentrum Jülich, Jülich, Germany. ⁴University of Barcelona, Barcelona, Spain. ⁵Simons Initiative for the Developing Brain, University of Edinburgh, Edinburgh, UK. ⁶Dementia Research Institute, University of Edinburgh, Edinburgh, UK. ✉email: Oksana.Sorokina@ed.ac.uk; Colin.D.Mclean@ed.ac.uk

Study name	Gene_N	Compartment	Brain region	Species
Husi_2000[1]	77	postsynaptic	forebrain	mouse
Walikonis_2000[2]	29	postsynaptic	forebrain	rat
Peng_2004[3]	237	postsynaptic	forebrain	rat
Satoh_2002[4]	45	postsynaptic	forebrain	mouse
Youshimura_2004[5]	436	postsynaptic	forebrain	rat
Farr_2004[6]	73	postsynaptic	whole brain	rat
Jordan_2004[7]	393	postsynaptic	whole brain	mouse and rat
Li_2004[8]	139	postsynaptic	forebrain	rat
Trinidad_2005[9]	236	postsynaptic	whole brain	mouse
Cheng_2006[10]	289	postsynaptic	forebrain and cerebellum	rat
Collins_2006[11]	620	postsynaptic	forebrain	mouse
Dosemeci_2006[12]	114	postsynaptic	hippocampus	rat
Dosemeci_2007[13]	276	postsynaptic	cerebral cortex	rat
Trinidad_2008[14]	2158	postsynaptic	cortex, midbrain, cerebellum, and hippocampus	mouse
Selimi_2009[15]	63	postsynaptic	cerebellum	mouse
Fernandez_2009[16]	113	postsynaptic	forebrain	mouse
Bayes_2011[17]	1443	postsynaptic	cortex	human
Bayes_2012[18]	1552	postsynaptic	cortex	mouse
Schwenk_2013[19]	34	postsynaptic	whole brain	mouse
Distler_2014[20]	3558	postsynaptic	hippocampus	mouse
Bayes_2014[21]	1134	postsynaptic	frontal cortex	human
Uezu_2016[22]	928	postsynaptic	cortex and hippocampus	mouse
Focking_2016[23]	2021	postsynaptic	whole brain	human
Li_2016[24]	1602	postsynaptic	hippocampus CA1	mouse
Fernandez_2017[25]	107	postsynaptic	forebrain	mouse
Roy_2017[26]	1213	postsynaptic	frontal, parietal, temporal and occipital lobes of the neocortex	human
Li_2017[27]	993	postsynaptic	hippocampus CA1	mouse
Roy_2018[28]	1071	postsynaptic	frontal, medial and caudal cortex, right caudate putamen, right hippocampus, whole hypothalamus, and cerebellum (right half)	mouse
Wilson_2019[29]	2134	postsynaptic	cortex	mouse
Coughenour_2004[30]	36	presynaptic	forebrain	rat
Blondeau_2004[31]	209	presynaptic	whole brain	rat
Phillips_2005[32]	110	presynaptic	cortex	rat

Table 1. (continued)

Morciano_2005[33]	153	presynaptic	whole brain	rat
Burre_2006[34]	165	presynaptic	whole brain	rat
Takamori_2006[35]	410	presynaptic	cerebral cortex	rat
Khanna_2007[36]	104	presynaptic	whole brain	rat
Morciano_2009[37]	369	presynaptic	whole brain	rat
Abul-Husn_2009[38]	138	presynaptic	hippocampus and striatum	mouse
Abul-Husn_2011[39]	145	presynaptic	striatum	rat
Gorini_2010[40]	57	presynaptic	cortex	mouse
Gronborg_2010[41]	618	presynaptic	cerebral cortex	rat
Boyken_2013[42]	414	presynaptic	cerebral cortex	rat
Wilhelm_2014[43]	1169	presynaptic	cortex and cerebellum	rat
Brinkmalm_2014[44]	68	presynaptic	hippocampus	mouse
Weingarten_2014[45]	482	presynaptic	whole brain	mouse
Kokotos_2018[46]	983	presynaptic	cerebellum	rat
Taoufiq_2020[47]	1,466	presynaptic	whole brain	rat
Filiou_2010[48]	2980	synaptosome	whole brain	mouse
Dahlhaus_2011[49]	673	synaptosome	visual cortex	mouse
Cohen_2013[50]	2668	synaptosome	cortex	rat
Biesemann_2014[51]	163	synaptosome	forebrain	mouse
Chang_2015[52]	2077	synaptosome	cortex	human
Liu_2014[53]	1388	synaptosome	hippocampus and prefrontal cortex	mouse
Distler_2014[20]	4417	synaptosome	hippocampus	mouse
Kohansal-Nodehi_2016[54]	4961	synaptosome	cerebellum	rat
Gonzalez-Lozano[55]	1560	synaptosome	cortex	mouse
Alfieri_2017[56]	351	synaptosome	telencephalon	mouse
Heo_2018[57]	2272	synaptosome	cortex and hippocampus	mouse
Taoufiq_2020[47]	4,439	synaptosome	whole brain	rat

Table 1. Studies included in the database. Dark grey corresponds to postsynaptic, light grey—to presynaptic, and green—to synaptosomal studies.

DIP⁶⁰. The resulting PSP network contains 4817 nodes and 27,788 edges in the Largest Connected Component (LCC). The presynaptic network is significantly smaller and comprises 2221 nodes and 8678 edges in the LCC.

The resulting network model is embedded into a SQLite implementation allowing users to derive custom network models based on meta-data including species, disease association, synaptic compartment, brain region, and method of extraction (Fig. 2). The database with manual is available from Supplementary Materials and from Edinburgh DataShare <https://doi.org/10.7488/ds/3017>, along with a SQLite Studio manual and Rmd file for querying under the R environment, a screencast walk-through demonstrating use-cases can also be found here <https://youtu.be/oaW9Yr9AkXM>.

The dataset can be used to answer frequent questions such as “What is known about my favourite gene? Is it pre- or postsynaptic? Which brain region was it identified in?”. Beyond that, users can extend these queries to extract custom networks based on bespoke subsets of molecules. Worked examples that are easy to customise are shown in the Supplementary files.

The underlying principle of a systems biology approach is that structural features (pathways and subnetworks) underpin network functionality and given a network, one should be able to extract these features. Clustering algorithms^{61,62} are commonly used to identify local communities within the network under the assumption that shared network topology correlates with shared function (and dysfunction). However, the

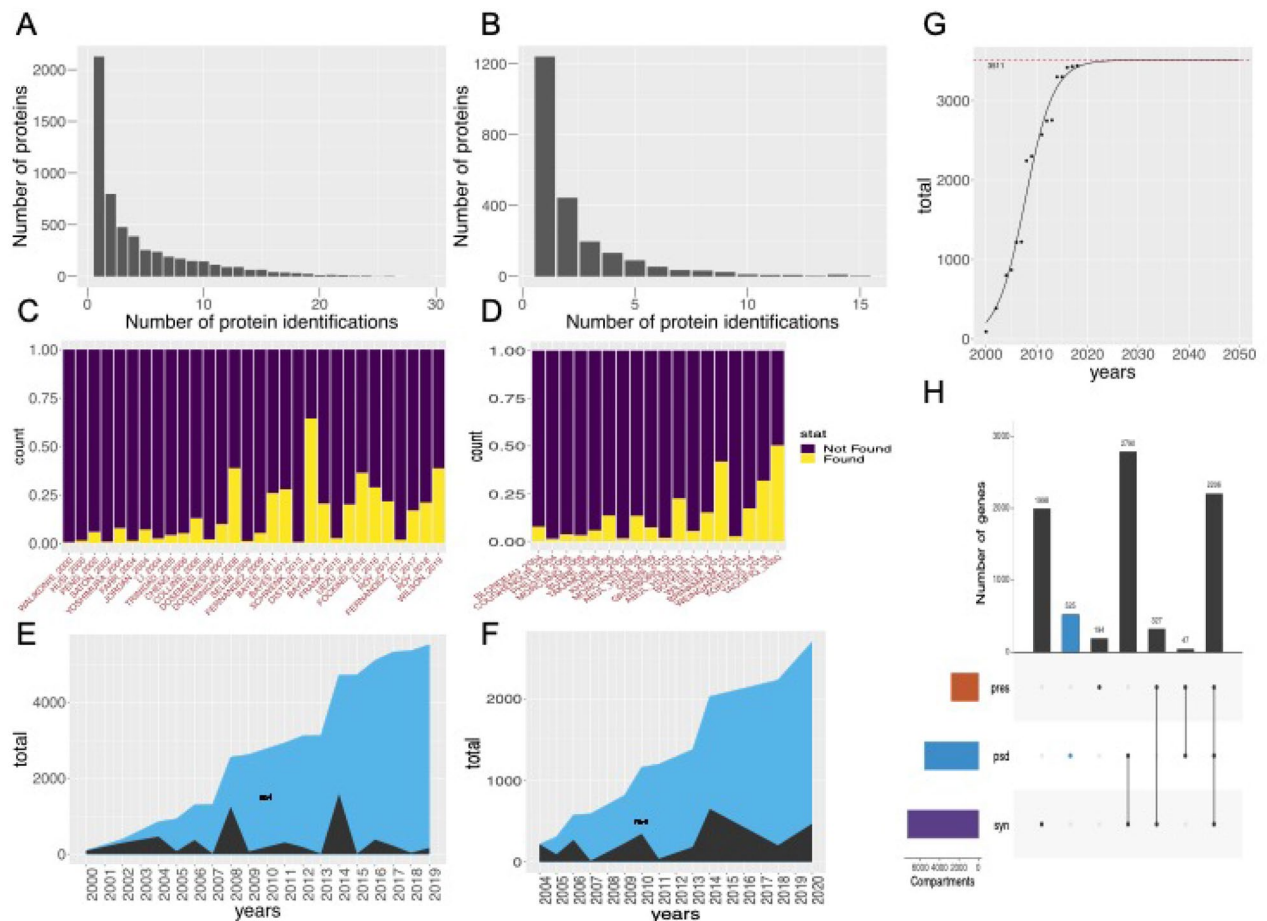


Figure 1. (A) Discovery rate of new PSD proteins across 29 postsynaptic studies, where the number of proteins is plotted against the frequency of identification. 2091 PSP proteins have been observed just once. The most frequently found proteins (i.e. detected in 22, or more, studies out of the 29) include very well-known PSD proteins, for example: DLG4 (28/29), CAMK2A (27/29), INA (26/29), SPTBN1, CAMK2B, DLG2, NSF, GRIN2B, GRIN1 (25/29), BIAP2, BSN (24/29) (full list in Supplementary Table 2). (B) Discovery rate of new proteins analysed across 18 presynaptic studies. More than half of the proteins in the presynaptic proteome (1251) have been observed just once. The most frequent presynaptic genes include AP2B1, HSPA8, GNAO1, ACTB (15/17), STX1B, ATP6V0A1, STXBP1, ATP1A3, ATP6V1E1, SYT1, GNB1, TUBA1A, VAMP2, NSF, DNMI (14/17) with full statistics available in Supplementary Table 3. (C) Contribution of each of 29 studies to the total number of PSP genes (purple—total number of genes, yellow—identified in this study). Two major jumps in the gross number of proteins identified occur in 2008, when 1249 new proteins were reported by¹⁴ and in 2014 with 2588 new proteins added by²⁰. (D) Contribution of each of 18 studies to the total number of presynaptic genes (purple—total number of genes, yellow—identified in this study): two jumps in newly discovered proteins correspond to studies in years 2010 and 2014. (E) Accumulation of the new PSD genes (black) compared to the total datasets (blue) over years. (F) Accumulation of new presynaptic genes (black) compared to the total datasets (blue) over years. (G) Non-linear fit predicting the total size of “consensus” PSP (genes found in two and more studies, 3499) ($P = 2.36 \times 10^{-11}$, residual standard error: 192.7 on 12 degrees of freedom) by year 2023 which, when compared to the current number (3438) indicates that our knowledge on PSP components, based on currently available methodologies, is close to saturation. (H) Overlap of three synaptic datasets: presynaptic, postsynaptic and synaptosomal. Bars correspond to the number of unique genes in each compartment and their intersections.

more important question is how the different communities are organised to enable a controllable flow of signals across the large network. Using the PSP network as example, we identified 1029 “Bridging” proteins as those known to interact locally with neighbours in the network—helping organise function inside communities they belong to^{63,64}, and simultaneously influence other communities in the network (Fig. 3A, Methods). Using graph entropy as a complement means of ranking a protein’s ability to inhibit or enhance information flow⁶⁵, we found that proteins with high Bridgeness value have ability to decrease the entropy of the network thus facilitating the signal transmission (Fig. 3B,D, Methods). Of the 1029 candidate Bridging proteins (see Region 1, Fig. 3C), we found ~43% associated with at least one known synaptopathy and ~21% linked to multiple diseases including: APP (AD&Epi&ASD&PD&HTN&MS&FTD), VDAC1 (AD&PD&MS), and MAPK14

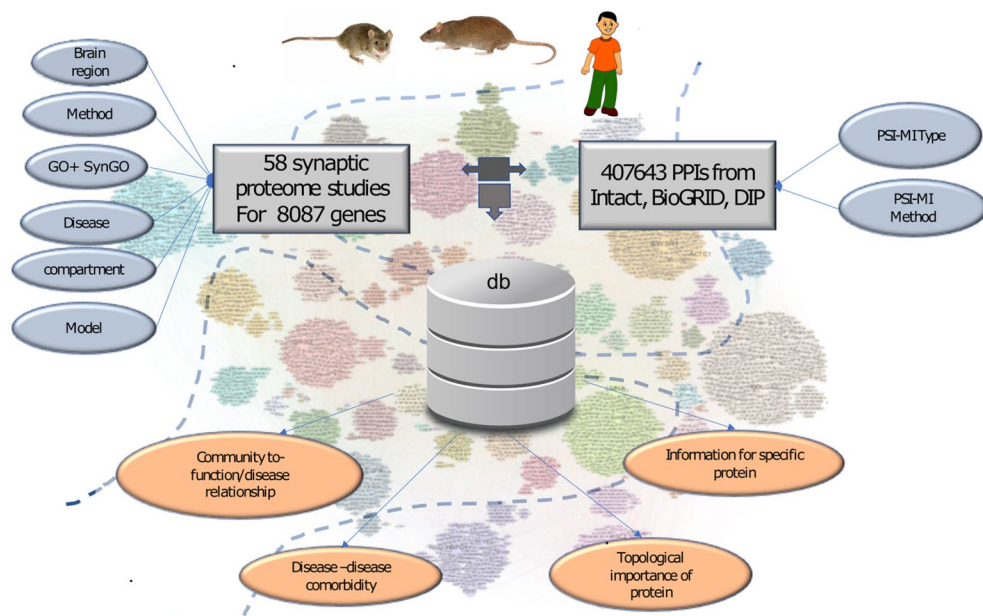


Figure 2. Structure of the SQLite database, which includes 58 synaptic studies covering 8087 unique genes and 407,643 direct protein interactions. Grey ovals on the top show the annotated metadata: left—for nodes/genes, which include brain region, subcellular compartment, method of extraction, disease and GO function annotation and link to published quantitative models; right—for edges/PPIs, which include PSI-MI type and method. The orange ovals in the bottom illustrate the possible outcomes of the database, including: (1) information for specific protein/gene, and (2) information that could be obtained from PPI network, e.g., protein's topological importance, community to disease relationship, and disease-disease comorbidity. The database is available as a Supplementary File and from Edinburgh DataShare <https://doi.org/10.7488/ds/3017>.

(AD&SCH&HD&HTN&MS), which supports the functional/disease importance of “bridging” proteins. Indeed, we found significant overrepresentation for specific diseases, such as AD ($P = 3.4 \times 10^{-6}$), HTN ($P = 2.1 \times 10^{-5}$), HD ($P = 5.2 \times 10^{-5}$), PD ($P = 2.6 \times 10^{-3}$) (Supplementary Table 2).

There are many complex co-morbidities between psychiatric disorders at the population and the genetic level but for most the molecular basis remains elusive. The network perspective can be used to obtain a different view by linking topology and phenotype together. Gene-disease association data is noisy and far from complete, but we can partly compensate by measuring, for each disease, the distance from each protein in the network to its nearest known associated protein, which can be extended to disease pairs⁶⁶ to dissect how these different neurological diseases coalesce at the synapse.

Using PSP (both full and consensus) and presynaptic networks we found clear evidence of network overlap between well-known co-morbid neuro-psychiatric/developmental disorders in both postsynaptic and presynaptic models (q-values shown for PSP/presynaptic networks), including BD-SCH ($P = 2.0 \times 10^{-49}/4.39 \times 10^{-16}$), BD-ASD ($P = 7.12 \times 10^{-20}/1.28 \times 10^{-7}$), and ASD/SCH ($P = 6.17 \times 10^{-16}/1.12 \times 10^{-5}$). Similarly, overlap was observed for common neurodegenerative diseases/conditions AD and PD ($P = 3.04 \times 10^{-6}/1.32 \times 10^{-6}$).

We also observed compartment-specific overlaps for Epilepsy with PD ($P = 0.53/2.12 \times 10^{-3}$) and BD ($P = 0.54/9.73 \times 10^{-4}$), which is significant only in the presynaptic network (Fig. 3E).

In both postsynaptic and presynaptic models, we found overlap for Hypertension (HTN) with AD ($P = 8.6 \times 10^{-4}/1.0 \times 10^{-2}$, and with MS ($P = 8.79 \times 10^{-5}/2.12 \times 10^{-3}$) (Fig. 3E). The AD-HTN link is not, in itself, new but commonly considered as a cardiovascular mechanism with a neurological impact. However, the network view reveals a new potential mechanistic link at the synapse. Although we found significant overlaps between AD-HTN and AD-PD, we did not see evidence for a PD-HTN link ($P = 0.17/0.36$), which indicates the potential shared mechanistic pathway between AD and HTN, which is different to the pathways shared between AD and PD (Fig. 3E).

To further dissect the potential sharing of pathways between AD and HTN in the PSP network (Fig. 3F), we employed Belief Propagation to propagate these GDA's through the network's edges, and a Degree-Corrected Block Model (DC-SBM) to model its effect on network clustering⁶⁷. Under a prior assumption of no correlation between the GDA's and the network communities, we found evidence for the co-localization of AD and HTN ($C = 31$ $P = 4.69 \times 10^{-5}$ and $C = 43$ $P = 1.6 \times 10^{-11}$). Functionally, these communities are enriched for synaptic transmission, axon guidance ($C = 31$, GO:0007268 = 5.8×10^{-3} , GO:0007411 = 7.46×10^{-5}), stress activated MAPK cascade and response to oxidative stress ($C = 43$, GO:0051403 = 1.92×10^{-5} , GO:0006979 = 5.34×10^{-5}).

The presented synapse proteome dataset is the largest, most complete and up to date and is freely available with lightweight tools to allow anyone to extract relevant subsets. It compliments previously published curated dataset of synaptic genes SynGO⁶⁸, and both resources could be used jointly as we have cross-referenced the

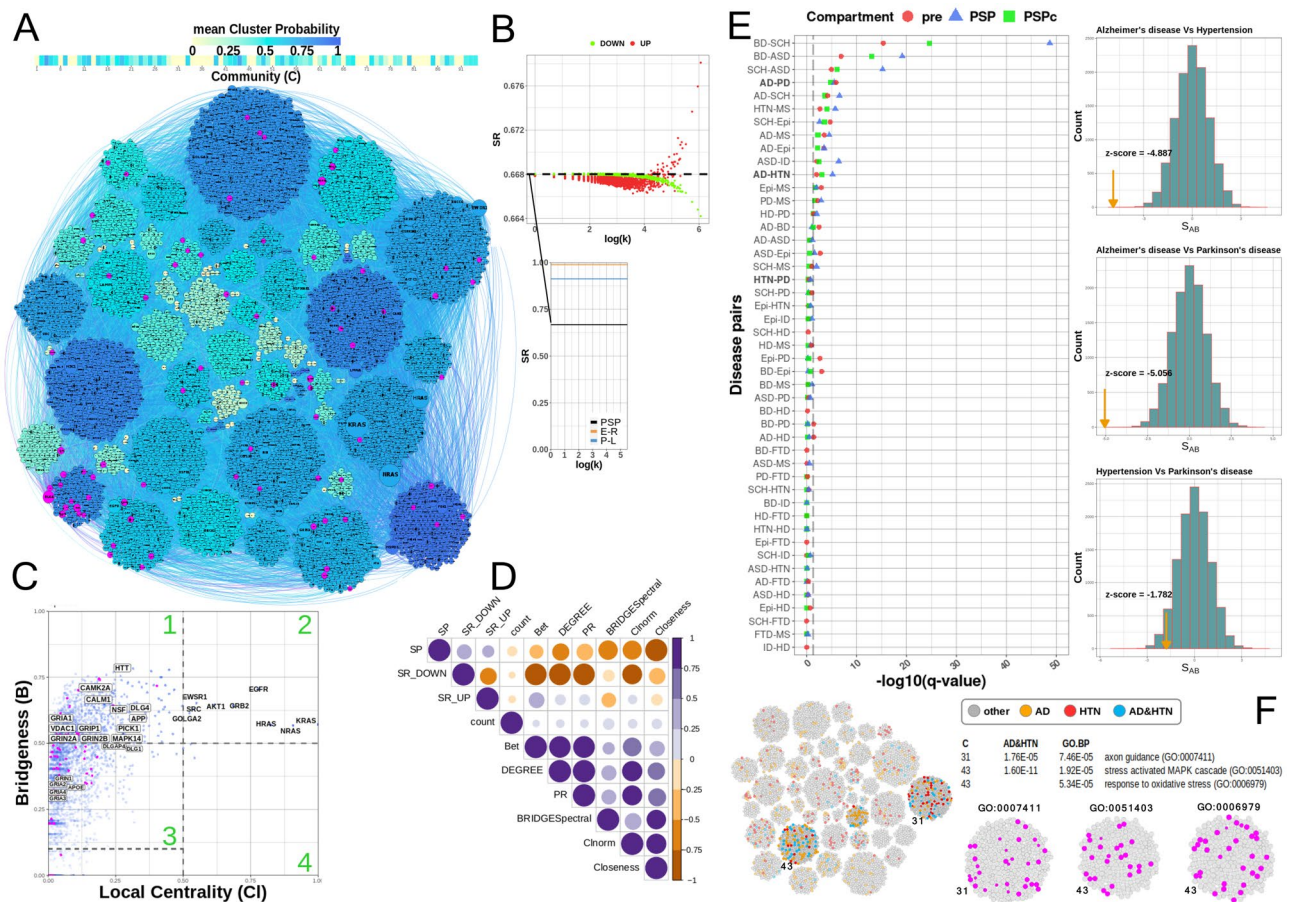


Figure 3. (A) Community structure of the PSP network using the Spectral modularity method. Communities are coloured using the average gene-community probability values: bluer coloured a community is, the more probable the genes are of belonging to that community on average. Nodes coloured magenta highlight the core PSD95 interactors²⁵, which is also highlighted magenta in the Bridgeness plot in (C). (B) Graph entropy plots: (main) Global graph entropy rate (SR) plot comparing the structure of the PSP network (0.668) against 1000 randomised Erdős–Rényi (E–R = 0.989 + − 0.0005) and Power–Law (P–L = 0.9127 + − 0.0032, $\alpha_{PSP} = 2.41$) models of similar size, (Enlarged) Evidence for scale-free structure in PSP network using a perturbation analysis [10], plotted is the SR values after each protein is perturbed through over-expression (SR_UP = red) and under-expression (SR_DOWN = green), against the log of the proteins degree. (C) Bridging proteins, estimated using the Spectral clustering algorithm are plotted against semi-local centrality (Methods), allowing their categorisation: Region 1, proteins having a 'global' rather than 'local' influence in the network (also been called bottle-neck bridges, connector or kinless hubs¹² (DLG4, GRIN2B, CAMK2A, etc.). Region 2, proteins having 'global' and 'local' influence (EGFR, HRAS, NRAS, etc.). Region 3, proteins centred within the community they belong to, but also communicating with a few other specific communities (GRIN1, GRIA2-4). Region 4, proteins with 'local' impact, primarily within one or two communities (local or party hubs⁹). (D) Correlation plot for different centrality measures estimated for PSP network: SP - a protein's shortest path value, SR_UP - Entropy rate when protein is over expressed, SR_DOWN - entropy rate when protein is under expressed, COUNT - number of protein identifications in the studies, Bet - protein's betweenness centrality value, Degree - protein degree, PR - Page Rank, BRIDGESpectral - protein Bridgeness value, CNorm - Protein's local centrality value, Closeness - protein's closeness value; correlation between SR_UP and Bridgeness indicates that genes with higher Bridgeness values also lower the graphs entropy when active/overexpressed, which allows the signal to pass more freely (Supplementary Table 2). (E) left: Disease-disease relationship for presynaptic (red) and PSD full (blue) and PSD consensus (green) interactome. Where significance q-values < 0.05 is delineated by the dashed line. Schizophrenia (SCH), Autistic Spectrum Disorder (ASD), Autistic Disorder (AUT), Bipolar Disorder (BD), Intellectual Disability (ID), Alzheimer disease (AD), Epilepsy Syndrome (Epi), Parkinson's Disease (PD), Frontotemporal Dementia (FTD), Huntington's Disease (HD) and Multiple Sclerosis (MS) are considered; right: randomisation studies for disease-disease pairs overlap, yellow arrow shows the measured value of Z-score compared to 10,000 AD-HTN, PD-HTN and AD-PD random models. (F) Colocalization of AD and HTN on the PSP network by propagating these gene-disease associations (GDA) through the network using the Belief Propagation DC-SBM algorithm¹³. The colocalization of AD and HTN shared common molecular pathways in communities 31 and 43, which were also found enriched for axon guidance, stress-activated MAPK cascade and response to oxidative stress GO BP terms.

common genes. By mirroring the methods used it would be straightforward for any user to add in their own datasets for comparison.

Received: 5 February 2021; Accepted: 15 April 2021

Published online: 11 May 2021

References

- Husi, H. *et al.* Proteomic analysis of NMDA receptor-adhesion protein signaling complexes. *Nat. Neurosci.* **3**(7), 661–669 (2000).
- Walikonis, R. S. *et al.* Identification of proteins in the postsynaptic density fraction by mass spectrometry. *J. Neurosci.* **20**(11), 4069–4080 (2000).
- Peng, J. *et al.* Semiquantitative proteomic analysis of rat forebrain postsynaptic density fractions by mass spectrometry. *J. Biol. Chem.* **279**(20), 21003–21011 (2004).
- Satoh, K. *et al.* Identification of activity-regulated proteins in the postsynaptic density fraction. *Genes Cells* **7**(2), 187–197 (2002).
- Yoshimura, Y. *et al.* Molecular constituents of the postsynaptic density fraction revealed by proteomic analysis using multidimensional liquid chromatography-tandem mass spectrometry. *J. Neurochem.* **88**(3), 759–768 (2004).
- Farr, C. D. *et al.* Proteomic analysis of native metabotropic glutamate receptor 5 protein complexes reveals novel molecular constituents. *J. Neurochem.* **91**(2), 438–450 (2004).
- Jordan, B. A. *et al.* Identification and verification of novel rodent postsynaptic density proteins. *Mol. Cell Proteom.* **3**(9), 857–871 (2004).
- Li, K. W. *et al.* Proteomics analysis of rat brain postsynaptic density. Implications of the diverse protein functional groups for the integration of synaptic physiology. *J. Biol. Chem.* **279**(2), 987–1002 (2004).
- Trinidad, J. C. *et al.* Phosphorylation state of postsynaptic density proteins. *J. Neurochem.* **92**(6), 1306–1316 (2005).
- Cheng, D. *et al.* Relative and absolute quantification of postsynaptic density proteome isolated from rat forebrain and cerebellum. *Mol. Cell Proteom.* **5**(6), 1158–1170 (2006).
- Collins, M. O. *et al.* Molecular characterization and comparison of the components and multiprotein complexes in the postsynaptic proteome. *J. Neurochem.* **97**(Suppl 1), 16–23 (2006).
- Dosemeci, A. *et al.* Preparation of postsynaptic density fraction from hippocampal slices and proteomic analysis. *Biochem. Biophys. Res. Commun.* **339**(2), 687–694 (2006).
- Dosemeci, A. *et al.* Composition of the synaptic PSD-95 complex. *Mol. Cell Proteom.* **6**(10), 1749–1760 (2007).
- Trinidad, J. C. *et al.* Quantitative analysis of synaptic phosphorylation and protein expression. *Mol. Cell Proteom.* **7**(4), 684–696 (2008).
- Selimi, F. *et al.* Proteomic studies of a single CNS synapse type: The parallel fiber/purkinje cell synapse. *PLoS Biol.* **7**(4), e83 (2009).
- Fernandez, E. *et al.* Targeted tandem affinity purification of PSD-95 recovers core postsynaptic complexes and schizophrenia susceptibility proteins. *Mol. Syst. Biol.* **5**, 269 (2009).
- Bayes, A. *et al.* Characterization of the proteome, diseases and evolution of the human postsynaptic density. *Nat. Neurosci.* **14**(1), 19–21 (2011).
- Bayes, A. *et al.* Comparative study of human and mouse postsynaptic proteomes finds high compositional conservation and abundance differences for key synaptic proteins. *PLoS ONE* **7**(10), e46683 (2012).
- Schwenk, J. *et al.* High-resolution proteomics unravel architecture and molecular diversity of native AMPA receptor complexes. *Neuron* **74**(4), 621–633 (2012).
- Distler, U. *et al.* In-depth protein profiling of the postsynaptic density from mouse hippocampus using data-independent acquisition proteomics. *Proteomics* **14**(21–22), 2607–2613 (2014).
- Bayes, A. *et al.* Human post-mortem synapse proteome integrity screening for proteomic studies of postsynaptic complexes. *Mol. Brain* **7**, 88 (2014).
- Seo, T. K. & Thorne, J. L. Information criteria for comparing partition schemes. *Syst. Biol.* **67**(4), 616–632 (2018).
- Focking, M. *et al.* Proteomic analysis of the postsynaptic density implicates synaptic function and energy pathways in bipolar disorder. *Transl. Psychiatry* **6**(11), e959 (2016).
- Li, J. *et al.* Long-term potentiation modulates synaptic phosphorylation networks and reshapes the structure of the postsynaptic interactome. *Sci. Signal.* **9**(440), 8 (2016).
- Fernandez, E. *et al.* Arc requires PSD95 for assembly into postsynaptic complexes involved with neural dysfunction and intelligence. *Cell Rep.* **21**(3), 679–691 (2017).
- Roy, M. *et al.* Proteomic analysis of postsynaptic proteins in regions of the human neocortex. *Nat. Neurosci.* **21**(1), 130–138 (2018).
- Li, J. *et al.* Spatiotemporal profile of postsynaptic interactomes integrates components of complex brain disorders. *Nat. Neurosci.* **20**(8), 1150–1161 (2017).
- Roy, M. *et al.* Regional diversity in the postsynaptic proteome of the mouse brain. *Proteomes* **6**, 3 (2018).
- Wilson, R. S. *et al.* Development of targeted mass spectrometry-based approaches for quantitation of proteins enriched in the postsynaptic density (PSD). *Proteomes* **7**, 2 (2019).
- Coughenour, H. D., Spaulding, R. S. & Thompson, C. M. The synaptic vesicle proteome: A comparative study in membrane protein identification. *Proteomics* **4**(10), 3141–3155 (2004).
- Blondeau, F. *et al.* Tandem MS analysis of brain clathrin-coated vesicles reveals their critical involvement in synaptic vesicle recycling. *Proc. Natl. Acad. Sci. U.S.A.* **101**(11), 3833–3838 (2004).
- Phillips, G. R. *et al.* Proteomic comparison of two fractions derived from the transsynaptic scaffold. *J. Neurosci. Res.* **81**(6), 762–775 (2005).
- Morciano, M. *et al.* Immunolocalization of two synaptic vesicle pools from synaptosomes: A proteomics analysis. *J. Neurochem.* **95**(6), 1732–1745 (2005).
- Burre, J. *et al.* Analysis of the synaptic vesicle proteome using three gel-based protein separation techniques. *Proteomics* **6**(23), 6250–6262 (2006).
- Takamori, S. *et al.* Molecular anatomy of a trafficking organelle. *Cell* **127**(4), 831–846 (2006).
- Khanna, R., Zougman, A. & Stanley, E. F. A proteomic screen for presynaptic terminal N-type calcium channel (CaV2.2) binding partners. *J. Biochem. Mol. Biol.* **40**(3), 302–314 (2007).
- Morciano, M. *et al.* The proteome of the presynaptic active zone: From docked synaptic vesicles to adhesion molecules and maxi-channels. *J. Neurochem.* **108**(3), 662–675 (2009).
- Abul-Husn, N. S. *et al.* Systems approach to explore components and interactions in the presynapse. *Proteomics* **9**(12), 3303–3315 (2009).
- Abul-Husn, N. S. *et al.* Chronic morphine alters the presynaptic protein profile: Identification of novel molecular targets using proteomics and network analysis. *PLoS ONE* **6**(10), e25535 (2011).
- Gorini, G. *et al.* Dynamin-1 co-associates with native mouse brain BKCa channels: Proteomics analysis of synaptic protein complexes. *FEBS Lett.* **584**(5), 845–851 (2010).

41. Gronborg, M. *et al.* Quantitative comparison of glutamatergic and GABAergic synaptic vesicles unveils selectivity for few proteins including MAL2, a novel synaptic vesicle protein. *J. Neurosci.* **30**(1), 2–12 (2010).
42. Boyken, J. *et al.* Molecular profiling of synaptic vesicle docking sites reveals novel proteins but few differences between glutamatergic and GABAergic synapses. *Neuron* **78**(2), 285–297 (2013).
43. Wilhelm, B. G. *et al.* Composition of isolated synaptic boutons reveals the amounts of vesicle trafficking proteins. *Science* **344**(6187), 1023–1028 (2014).
44. Brinkmalm, A. *et al.* Targeting synaptic pathology with a novel affinity mass spectrometry approach. *Mol. Cell Proteom.* **13**(10), 2584–2592 (2014).
45. Weingarten, J. *et al.* The proteome of the presynaptic active zone from mouse brain. *Mol. Cell Neurosci.* **59**, 106–118 (2014).
46. Kokotos, A. C. *et al.* Activity-dependent bulk endocytosis proteome reveals a key presynaptic role for the monomeric GTPase Rab11. *Proc. Natl. Acad. Sci. U.S.A.* **115**(43), E10177–e10186 (2018).
47. Taoufiq, Z. *et al.* Hidden proteome of synaptic vesicles in the mammalian brain. *Proc. Natl. Acad. Sci. U.S.A.* **117**(52), 33586–33596 (2020).
48. Filiou, M. D. *et al.* Profiling of mouse synaptosome proteome and phosphoproteome by IEF. *Electrophoresis* **31**(8), 1294–1301 (2010).
49. Dahlhaus, M. *et al.* The synaptic proteome during development and plasticity of the mouse visual cortex. *Mol. Cell Proteom.* **10**(5), 5413 (2011).
50. Cohen, L. D. *et al.* Metabolic turnover of synaptic proteins: Kinetics, interdependencies and implications for synaptic maintenance. *PLoS ONE* **8**(5), e63191 (2013).
51. Biesemann, C. *et al.* Proteomic screening of glutamatergic mouse brain synaptosomes isolated by fluorescence activated sorting. *Embo J.* **33**(2), 157–170 (2014).
52. Chang, R. Y. *et al.* SWATH analysis of the synaptic proteome in Alzheimer's disease. *Neurochem. Int.* **87**, 1–12 (2015).
53. Liu, X. A. *et al.* New approach to capture and characterize synaptic proteome. *Proc. Natl. Acad. Sci. U.S.A.* **111**(45), 16154–16159 (2014).
54. Kohansal-Nodehi, M. *et al.* Analysis of protein phosphorylation in nerve terminal reveals extensive changes in active zone proteins upon exocytosis. *Elife* **5**, 2 (2016).
55. Gonzalez-Lozano, M. A. *et al.* Dynamics of the mouse brain cortical synaptic proteome during postnatal brain development. *Sci. Rep.* **6**, 35456 (2016).
56. Alfieri, A. *et al.* Synaptic interactome mining reveals p140Cap as a new hub for PSD proteins involved in psychiatric and neurological disorders. *Front. Mol. Neurosci.* **10**, 212 (2017).
57. Heo, S. *et al.* Identification of long-lived synaptic proteins by proteomic analysis of synaptosome protein turnover. *Proc. Natl. Acad. Sci. U.S.A.* **115**(16), E3827–e3836 (2018).
58. Oughtred, R. *et al.* The BioGRID interaction database: 2019 update. *Nucleic Acids Res.* **47**(D1), D529–d541 (2019).
59. Kerrien, S. *et al.* The IntAct molecular interaction database in 2012. *Nucleic Acids Res.* **40**, 841–846 (2012).
60. Xenarios, I. *et al.* DIP, the database of interacting proteins: A research tool for studying cellular networks of protein interactions. *Nucleic Acids Res.* **30**(1), 303–305 (2002).
61. Newman, M. E. Modularity and community structure in networks. *Proc. Natl. Acad. Sci. U.S.A.* **103**(23), 8577–8582 (2006).
62. McLean, C. *et al.* Improved functional enrichment analysis of biological networks using scalable modularity based clustering. *J. Proteom. Bioinform.* **9**(1), 9–18 (2016).
63. Han, J. D. *et al.* Evidence for dynamically organized modularity in the yeast protein–protein interaction network. *Nature* **430**(6995), 88–93 (2004).
64. Nepusz, T., Yu, H. & Paccanaro, A. Detecting overlapping protein complexes in protein–protein interaction networks. *Nat. Methods* **9**(5), 471–472 (2012).
65. Teschendorff, A. E. *et al.* Increased signaling entropy in cancer requires the scale-free property of protein interaction networks. *Sci. Rep.* **5**, 9646 (2015).
66. Menche, J. *et al.* Disease networks. Uncovering disease–disease relationships through the incomplete interactome. *Science* **347**(6224), 1257601 (2015).
67. Newman, M. E. & Clauset, A. Structure and inference in annotated networks. *Nat. Commun.* **7**, 11863 (2016).
68. Koopmans, F. *et al.* SynGO: An evidence-based, expert-curated knowledge base for the synapse. *Neuron* **103**(2), 217–234.e4 (2019).

Acknowledgements

We would like to thank Anatoly Sorokin for help with the database. This research has received funding from the European Union's Horizon 2020 Framework Programme for Research and Innovation under the Specific Grant Agreement Nos. 695568, 785907, 945539 (SYNNOVATE, Human Brain Project SGA02 and Human Brain Project SGA3), Wellcome Trust (Technology Development Grant 202932) and the Simons Initiative for the Developing Brain (SFARI—529085).

Author contributions

O.S., C.M., M.C., E.W., K.H., D.S., T.I.S. collected, reviewed and combined the datasets. C.M., O.S., X.H. performed the analysis. O.S. built the database. O.S., C.M. prepared Figs. 1, 2, 3. O.S., C.M., S.G. and J.D.A. wrote the manuscript. All authors reviewed the manuscript.

Competing interests

The authors declare no competing interests.

Additional information

Supplementary Information The online version contains supplementary material available at <https://doi.org/10.1038/s41598-021-88945-7>.

Correspondence and requests for materials should be addressed to O.S. or C.M.

Reprints and permissions information is available at www.nature.com/reprints.

Publisher's note Springer Nature remains neutral with regard to jurisdictional claims in published maps and institutional affiliations.



Open Access This article is licensed under a Creative Commons Attribution 4.0 International License, which permits use, sharing, adaptation, distribution and reproduction in any medium or format, as long as you give appropriate credit to the original author(s) and the source, provide a link to the Creative Commons licence, and indicate if changes were made. The images or other third party material in this article are included in the article's Creative Commons licence, unless indicated otherwise in a credit line to the material. If material is not included in the article's Creative Commons licence and your intended use is not permitted by statutory regulation or exceeds the permitted use, you will need to obtain permission directly from the copyright holder. To view a copy of this licence, visit <http://creativecommons.org/licenses/by/4.0/>.

© The Author(s) 2021